

# Spin-orbit torques in strained PtMnSb from first principles

Frank Freimuth<sup>1,2,\*</sup>, Stefan Blügel<sup>1</sup>, and Yuriy Mokrousov<sup>1,2</sup>

<sup>1</sup>*Peter Grünberg Institut and Institute for Advanced Simulation,*

*Forschungszentrum Jülich and JARA, 52425 Jülich, Germany and*

<sup>2</sup>*Institute of Physics, Johannes Gutenberg University Mainz, 55099 Mainz, Germany*

(Dated: January 27, 2023)

We compute spin-orbit torques (SOTs) in strained PtMnSb from first principles. We consider both tetragonal strain and shear strain. We find a strong linear dependence of the field-like SOTs on these strains, while the antidamping SOT is only moderately sensitive to shear strain and even insensitive to tetragonal strain. We also study the dependence of the SOT on the magnetization direction. In order to obtain analytical expressions suitable for fitting our numerical *ab-initio* results we derive a general expansion of the SOT in terms of all response tensors that are allowed by crystal symmetry. Our expansion includes also higher-order terms beyond the usually considered lowest order. We find that the dependence on the strain is much smaller for the higher-order terms than for the lowest order terms. In order to judge the sensitivity of the SOT on the exchange correlation potential we compute the SOT in both GGA and LDA. We find that the higher-order terms depend significantly on the exchange-correlation potential, while the lowest order terms are insensitive to it. Since the higher-order terms are small in comparison to the lowest order terms the total SOT is insensitive to the exchange correlation potential in strained PtMnSb.

## I. INTRODUCTION

The spin-orbit torque (SOT) allows us to switch the magnetization by electric current in noncentrosymmetric bulk crystals and in bilayers with structural inversion asymmetry [1]. It therefore paves the way to novel spintronic memory devices. Among the noncentrosymmetric bulk crystals the half-metallic half-Heusler compounds are promising for spintronics applications [2–5]. In particular, their high conduction-electron spin-polarization enhances for example the tunneling magnetoresistance and the giant magnetoresistance [6–9], and their half-metallicity suppresses the Gilbert damping [10].

The SOT in the half-Heusler NiMnSb depends strongly on the strain, which may be controlled by varying the substrate [11, 12]. Notably, NiMnSb thin films sputtered on GaAs substrates yield SOT effective fields per applied current that are similar in magnitude to those in Pt/Co/AlO<sub>x</sub> magnetic bilayers [13]. Tetragonal strain adds Dresselhaus spin-orbit interaction (SOI) to the microscopic half-Heusler Hamiltonian, while shear strain supplements it with both Rashba and Dresselhaus SOI.

The SOTs arising from Dresselhaus and Rashba SOI correspond to the lowest order in the expansion of the SOT with respect to the magnetization [14]. In magnetic bilayers the higher-order terms in this expansion have been found to be sizeable in experiments [15], and several theoretical works have therefore considered the dependence of the SOT on the magnetization direction in detail in these bilayer systems [16–18]. However, in the case of half-Heusler crystals the higher-order contributions in the expansion of the SOT in terms of the directional cosines of the magnetization have not yet been considered. Therefore, our symmetry analysis of the SOT

in this paper includes also the first higher-order terms in the directional cosine expansion. Such angular expansions may be used to fit experimental SOT data [15]. In the present paper we use the angular expansion in order to fit our *ab-initio* data, which allows us to separate the SOT into the lowest-order Dresselhaus and Rashba SOI contributions and the remaining higher-order terms.

PtMnSb is a promising material for spintronics applications. Its half-metallicity has been established both experimentally and theoretically. It can be grown epitaxially on MgO(001) [19] and on W(001)/MnO(001) [20]. It exhibits a giant magneto-optical Kerr effect [21, 22], which makes it attractive for magneto-optical recording. Furthermore, it exhibits a negative anisotropic magnetoresistance and it has been used for room-temperature giant magnetoresistance devices [23, 24]. In this paper we discuss the SOT in PtMnSb with tetragonal and shear strain obtained from first principles density-functional theory calculations.

This paper is structured as follows: In Sec. II we discuss the form of the SOT expected in half Heuslers based on the symmetry of the cubic, tetragonally strained, and shear-strained crystals. In Sec. III we present our *ab-initio* results on the SOTs in PtMnSb. In Sec. III A we describe the computational details. In Sec. III B we discuss the results on the odd torque and in Sec. III C we discuss the results on the even torque. This paper ends with a summary in Sec. IV.

## II. SYMMETRY OF SOTS IN HALF-HEUSLER CRYSTALS

The torque  $\mathbf{T}$  acting on the magnetization in one crystal unit cell is written as

$$\mathbf{T} = \sum_{ij} \hat{\mathbf{e}}_i t_{ij} \mathbf{E}_j, \quad (1)$$

\* Corresp. author: f.freimuth@fz-juelich.de

where  $t_{ij}$  is the torkance tensor,  $E_j$  is the  $j$ -th component of the applied electric field, and  $\hat{e}_i$  is a unit vector in the  $i$ -th Cartesian direction. We separate the torkance into even and odd parts with respect to inversion of the magnetization direction. The corresponding even SOT is often referred to as the antidamping SOT, while the odd SOT is often referred to as the field-like SOT.  $t_{ij}$  is an axial tensor of rank 2. It is possible to use the symmetries of the half-Heusler crystal in order to determine the form of  $t_{ij}$ . However, in practice only the torque perpendicular to the magnetization is of relevance. In general, an axial tensor of rank 2 consistent with the crystal symmetry may predict also a component of the torque that is parallel to the magnetization. In order to avoid this irrelevant component we consider first the effective magnetic field that one would have to apply in order to generate a torque of the same size as the SOT. For a given torque  $\mathbf{T}$  this effective magnetic field  $\mathbf{B}$  may be computed from

$$\mathbf{B} = \frac{\mathbf{T} \times \hat{\mathbf{M}}}{\mu}, \quad (2)$$

where  $\mu$  is the magnetic moment within one unit cell and  $\hat{\mathbf{M}}$  is its direction. When we use symmetry in order to determine the form of the response of  $\mathbf{B}$  to an applied electric field we may subsequently obtain the torque from  $\mathbf{T} = \mu \hat{\mathbf{M}} \times \mathbf{B}$ . This approach guarantees that the torque  $\mathbf{T}$  is perpendicular to the magnetization such that it is not necessary to remove irrelevant contributions obtained from symmetry analysis.

### A. Odd torque

The effective field of the odd torque can be expressed in terms of the electric field  $\mathbf{E}$  and the magnetization direction  $\hat{\mathbf{M}}$  as follows:

$$B_i^{\text{odd}} = \chi_{ij}^{(a)} E_j + \chi_{ijkl}^{(a)} E_j \hat{M}_k \hat{M}_l + \dots \quad (3)$$

Here,  $\chi_{ij}^{(a)}$  is an axial tensor of second rank,  $\chi_{ijkl}^{(a)}$  is an axial tensor of fourth rank and summation over repeated indices is implied. Note that the effective field of the odd torque is even in the magnetization. We introduce the notation

$$\delta_{ij}^{(mn)} = \delta_{im} \delta_{jn} \rightarrow \langle mn \rangle \quad (4)$$

and

$$\delta_{ijkl}^{(mnop)} = \delta_{im} \delta_{jn} \delta_{ko} \delta_{lp} \rightarrow \langle m nop \rangle. \quad (5)$$

TABLE I. List of axial tensors of ranks 2 and 4 allowed by symmetry in tetragonally strained half Heuslers. The notation introduced in Eq. (5) is used. Arrows indicate tensors that may be replaced by others due to permutations of indices, while (7) denotes tensors that may be replaced by others due to Eq. (7).

#	$\chi^{(a\#)}$	#	$\chi^{(a\#)}$	
1	$\langle 22 \rangle - \langle 11 \rangle$	7	$\langle 3113 \rangle - \langle 3223 \rangle$	$\rightarrow \chi^{(a5)}$
2	$\langle 2112 \rangle - \langle 1221 \rangle$	8	$\langle 2323 \rangle - \langle 1313 \rangle$	$\rightarrow \chi^{(a6)}$
3	$\langle 1122 \rangle - \langle 2211 \rangle$	9	$\langle 2233 \rangle - \langle 1133 \rangle$	
4	$\langle 3322 \rangle - \langle 3311 \rangle$	10	$\langle 1212 \rangle - \langle 2121 \rangle$	$\rightarrow -\chi^{(a2)}$
5	$\langle 3131 \rangle - \langle 3232 \rangle$	11	$\langle 2222 \rangle - \langle 1111 \rangle$	(7)
6	$\langle 2332 \rangle - \langle 1331 \rangle$			

### Tetragonal strain

First, we consider the case of tetragonal strain. For  $a = b \neq c$  and  $\alpha = \beta = \gamma = 90^\circ$  (point group  $\bar{4}2m$ ) we list the 11 axial tensors of rank 2 and 4 that are allowed by symmetry in Table I. In Eq. (3) the indices  $k$  and  $l$  of  $\chi_{ijkl}^{(a)}$  both couple to magnetization and are therefore interchangeable. Therefore, as indicated in Table I by arrows,

$$\begin{aligned} \chi_{ijkl}^{(a10)} &= -\chi_{ijlk}^{(a2)} \\ \chi_{ijkl}^{(a7)} &= \chi_{ijlk}^{(a5)} \\ \chi_{ijkl}^{(a8)} &= \chi_{ijlk}^{(a6)}. \end{aligned} \quad (6)$$

Moreover, we find

$$(\chi_{ijkl}^{(a3)} - \chi_{ijkl}^{(a9)} - \chi_{ijkl}^{(a11)}) \hat{M}_k \hat{M}_l = -\chi_{ij}^{(a1)}. \quad (7)$$

Thus, we do not need to consider the tensors 10, 7, 8 and 11 when we express  $\chi_{ijkl}^{(a)}$  in terms of the tensors in Table I. Consequently, we can express the tensors in Eq. (3) as

$$\begin{aligned} \chi_{ij}^{(a)} &= \alpha_1 \chi_{ij}^{(a1)} \\ \chi_{ijkl}^{(a)} &= \alpha_2 \chi_{ijkl}^{(a2)} + \alpha_3 \chi_{ijkl}^{(a3)} + \alpha_4 \chi_{ijkl}^{(a4)} + \\ &+ \alpha_5 \chi_{ijkl}^{(a5)} + \alpha_6 \chi_{ijkl}^{(a6)} + \alpha_7 \chi_{ijkl}^{(a9)} \end{aligned} \quad (8)$$

in terms of 7 expansion coefficients  $\alpha_1, \dots, \alpha_7$ . The tensor  $\chi_{ij}^{(a1)} = \delta_{ij}^{(22)} - \delta_{ij}^{(11)}$  describes the effective SOT field from Dresselhaus SOI [12, 14]. The tensors 2, 3, 4, 5, 6, and 9 describe higher-order contributions to the SOT, which have not yet been discussed in the literature.

The odd torque  $\mathbf{T}^{\text{odd}}$  is related to its effective field by

$$T_i^{\text{odd}} = \Xi_{ij} B_j^{\text{odd}}, \quad (9)$$

where

$$\Xi = \mu \begin{pmatrix} 0 & -\hat{M}_3 & \hat{M}_2 \\ \hat{M}_3 & 0 & -\hat{M}_1 \\ -\hat{M}_2 & \hat{M}_1 & 0 \end{pmatrix}. \quad (10)$$

Using Eq. (3), Eq. (8), and Eq. (9) we obtain

$$\mathbf{T}^{\text{odd}} = \mathbf{t}^{\text{odd}} \mathbf{E}, \quad (11)$$

where

$$t_{ij}^{\text{odd}} = \mu \sum_{k=1}^7 \alpha_k \vartheta_{ij}^{(\text{odd}k)} \quad (12)$$

with

$$\begin{aligned} \vartheta^{(\text{odd}1)} &= \begin{pmatrix} 0 & -\hat{M}_3 & 0 \\ -\hat{M}_3 & 0 & 0 \\ \hat{M}_2 & \hat{M}_1 & 0 \end{pmatrix} \\ \vartheta^{(\text{odd}2)} &= \begin{pmatrix} -\hat{M}_1 \hat{M}_2 \hat{M}_3 & 0 & 0 \\ 0 & -\hat{M}_1 \hat{M}_2 \hat{M}_3 & 0 \\ \hat{M}_1^2 \hat{M}_2 & \hat{M}_1 \hat{M}_2^2 & 0 \end{pmatrix} \\ \vartheta^{(\text{odd}3)} &= \begin{pmatrix} 0 & \hat{M}_1^2 \hat{M}_3 & 0 \\ \hat{M}_2^2 \hat{M}_3 & 0 & 0 \\ -\hat{M}_2^3 & -\hat{M}_1^3 & 0 \end{pmatrix} \\ \vartheta^{(\text{odd}4)} &= \begin{pmatrix} 0 & 0 & \hat{M}_2^3 - \hat{M}_1^2 \hat{M}_2 \\ 0 & 0 & \hat{M}_1^3 - \hat{M}_1 \hat{M}_2^2 \\ 0 & 0 & 0 \end{pmatrix} \quad (13) \\ \vartheta^{(\text{odd}5)} &= \begin{pmatrix} \hat{M}_1 \hat{M}_2 \hat{M}_3 & -\hat{M}_2^2 \hat{M}_3 & 0 \\ -\hat{M}_1^2 \hat{M}_3 & \hat{M}_1 \hat{M}_2 \hat{M}_3 & 0 \\ 0 & 0 & 0 \end{pmatrix} \\ \vartheta^{(\text{odd}6)} &= \begin{pmatrix} 0 & 0 & -\hat{M}_2 \hat{M}_3^2 \\ 0 & 0 & -\hat{M}_1 \hat{M}_3^2 \\ 0 & 0 & 2\hat{M}_1 \hat{M}_2 \hat{M}_3 \end{pmatrix} \\ \vartheta^{(\text{odd}7)} &= \begin{pmatrix} 0 & -\hat{M}_3^3 & 0 \\ -\hat{M}_3^3 & 0 & 0 \\ \hat{M}_3^2 \hat{M}_2 & \hat{M}_1 \hat{M}_3^2 & 0 \end{pmatrix}. \end{aligned}$$

Since

$$\vartheta^{(\text{odd}2)} + \vartheta^{(\text{odd}5)} - \vartheta^{(\text{odd}3)} + \vartheta^{(\text{odd}7)} = \vartheta^{(\text{odd}1)} \quad (14)$$

we can set  $\alpha_7 = 0$  in Eq. (12). Thus, the odd torkance tensor can be expressed in terms of 6 tensors  $\vartheta^{(\text{odd}1)}, \dots, \vartheta^{(\text{odd}6)}$ :

$$t_{ij}^{\text{odd}} = \sum_{k=1}^6 \beta_k \vartheta_{ij}^{(\text{odd}k)} \quad (15)$$

with expansion coefficients  $\beta_1, \dots, \beta_6$ . By fitting Eq. (15) to the odd torque given for a set of magnetization directions, one may determine the coefficients  $\beta_i$  and subsequently use Eq. (15) to predict the odd torque for any magnetization direction.

*Cubic PtMnSb*

Next, we discuss the odd torque for the case of cubic half Heuslers, i.e.,  $a = b = c$  and  $\alpha = \beta = \gamma = 90^\circ$

(point group  $\bar{4}3m$ ). In contrast to the case with tetragonal strain, symmetry does not allow axial tensors of rank 2 in cubic PtMnSb [14]. The following axial tensors of rank 4 are allowed by symmetry:

$$\begin{aligned} \chi_{ijkl}^{(\text{a}12)} &= \delta_{ijkl}^{(2121)} - \delta_{ijkl}^{(1212)} - \delta_{ijkl}^{(3131)} \\ &\quad + \delta_{ijkl}^{(3232)} + \delta_{ijkl}^{(1313)} - \delta_{ijkl}^{(2323)}, \\ \chi_{ijkl}^{(\text{a}13)} &= -\delta_{ijkl}^{(2211)} + \delta_{ijkl}^{(1122)} + \delta_{ijkl}^{(3311)} \\ &\quad - \delta_{ijkl}^{(3322)} - \delta_{ijkl}^{(1133)} + \delta_{ijkl}^{(2233)}, \\ \chi_{ijkl}^{(\text{a}14)} &= -\delta_{ijkl}^{(1221)} + \delta_{ijkl}^{(2112)} + \delta_{ijkl}^{(1331)} \\ &\quad - \delta_{ijkl}^{(2332)} - \delta_{ijkl}^{(3113)} + \delta_{ijkl}^{(3223)}. \end{aligned} \quad (16)$$

Since the indices  $k$  and  $l$  of  $\chi_{ijkl}$  both couple to magnetization in Eq. (3) and since

$$\chi_{ijkl}^{(\text{a}12)} \hat{M}_k \hat{M}_l = \chi_{ijkl}^{(\text{a}14)} \hat{M}_k \hat{M}_l \quad (17)$$

we do not need to consider  $\chi^{(\text{a}14)}$  when we expand  $\chi_{ijkl}^{(\text{a})}$  in terms of the tensors in Eq. (16). Comparison of these tensors to Table I yields

$$\begin{aligned} \chi_{ijkl}^{(\text{a}12)} &= \chi_{ijkl}^{(\text{a}2)} - \chi_{ijkl}^{(\text{a}5)} - \chi_{ijkl}^{(\text{a}6)}, \\ \chi_{ijkl}^{(\text{a}13)} &= \chi_{ijkl}^{(\text{a}3)} - \chi_{ijkl}^{(\text{a}4)} + \chi_{ijkl}^{(\text{a}9)}. \end{aligned} \quad (18)$$

Thus, for the cubic half Heuslers, we can express the tensors in Eq. (3) as follows:

$$\begin{aligned} \chi_{ij}^{(\text{a})} &= 0 \\ \chi_{ijkl}^{(\text{a})} &= \alpha_{12} \chi_{ijkl}^{(\text{a}12)} + \alpha_{13} \chi_{ijkl}^{(\text{a}13)}, \end{aligned} \quad (19)$$

with two coefficients  $\alpha_{12}$  and  $\alpha_{13}$  [14].

The corresponding torkance is given by

$$t_{ij}^{\text{odd}} = \mu \sum_{k=12}^{13} \alpha_k \vartheta_{ij}^{(\text{odd}k)} = \sum_{k=12}^{13} \beta_k \vartheta_{ij}^{(\text{odd}k)} \quad (20)$$

with

$$\begin{aligned} \vartheta^{(\text{odd}12)} &= \vartheta^{(\text{odd}2)} - \vartheta^{(\text{odd}5)} - \vartheta^{(\text{odd}6)} = \\ &\quad \begin{pmatrix} -2\hat{M}_1 \hat{M}_2 \hat{M}_3 & \hat{M}_2^2 \hat{M}_3 & \hat{M}_2 \hat{M}_3^2 \\ \hat{M}_1^2 \hat{M}_3 & -2\hat{M}_1 \hat{M}_2 \hat{M}_3 & \hat{M}_1 \hat{M}_3^2 \\ \hat{M}_1^2 \hat{M}_2 & \hat{M}_1 \hat{M}_2^2 & -2\hat{M}_1 \hat{M}_2 \hat{M}_3 \end{pmatrix} \end{aligned} \quad (21)$$

and

$$\begin{aligned} \vartheta^{(\text{odd}13)} &= \vartheta^{(\text{odd}3)} - \vartheta^{(\text{odd}4)} + \vartheta^{(\text{odd}7)} = \\ &\quad \begin{pmatrix} 0 & \hat{M}_1^2 \hat{M}_3 - \hat{M}_3^3 & -\hat{M}_2^3 + \hat{M}_1^2 \hat{M}_2 \\ \hat{M}_2^2 \hat{M}_3 - \hat{M}_3^3 & 0 & -\hat{M}_1^3 + \hat{M}_1 \hat{M}_2^2 \\ -\hat{M}_2^3 + \hat{M}_3^2 \hat{M}_2 & -\hat{M}_1^3 + \hat{M}_1 \hat{M}_3^2 & 0 \end{pmatrix}. \end{aligned} \quad (22)$$

Instead of using Eq. (20) to fit the odd torkance in cubic PtMnSb one can of course also use Eq. (15). By

equating Eq. (20) and Eq. (15) we find that in cubic PtMnSb the following relations should be satisfied:

$$\begin{aligned}\beta_1 &= -\beta_4, \\ 2\beta_1 &= \beta_3, \\ 2\beta_1 &= -\beta_2 - \beta_5, \\ \beta_6 &= \beta_1 + \beta_5.\end{aligned}\quad (23)$$

*Shear strain*

TABLE II. List of axial tensors of rank 2 and 4 allowed by symmetry in shear-strained half Heuslers. The notation introduced in Eq. (5) is used. Arrows indicate tensors that may be replaced by others due to permutation of indices, while (26) denotes tensors that may be replaced by others due to Eq. (26).

#	$\chi^{(a\#)}$	#	$\chi^{(a\#)}$	
1	$\langle 21 \rangle - \langle 12 \rangle$	12	$\langle 3132 \rangle - \langle 3231 \rangle$	(26)
2	$\langle 22 \rangle - \langle 11 \rangle$	13	$\langle 3232 \rangle - \langle 3131 \rangle$	(26)
3	$\langle 2121 \rangle - \langle 1212 \rangle$	14	$\langle 2332 \rangle - \langle 1331 \rangle$	
4	$\langle 2221 \rangle - \langle 1112 \rangle$	15	$\langle 2313 \rangle - \langle 1323 \rangle$	$\rightarrow 5$
5	$\langle 2331 \rangle - \langle 1332 \rangle$	16	$\langle 3123 \rangle - \langle 3213 \rangle$	$\rightarrow 12$
6	$\langle 2112 \rangle - \langle 1221 \rangle$	17	$\langle 3223 \rangle - \langle 3113 \rangle$	$\rightarrow 13$
7	$\langle 2212 \rangle - \langle 1121 \rangle$	18	$\langle 2323 \rangle - \langle 1313 \rangle$	$\rightarrow 14$
8	$\langle 3312 \rangle - \langle 3321 \rangle$	$\emptyset$	$\langle 2133 \rangle - \langle 1233 \rangle$	
9	$\langle 2122 \rangle - \langle 1211 \rangle$	19	$\langle 2233 \rangle - \langle 1133 \rangle$	
10	$\langle 2222 \rangle - \langle 1111 \rangle$	20	$\langle 2111 \rangle - \langle 1222 \rangle$	(26)
11	$\langle 3322 \rangle - \langle 3311 \rangle$	21	$\langle 2211 \rangle - \langle 1122 \rangle$	(26)
		22	$\langle 2211 \rangle - \langle 1122 \rangle$	(26)

Finally, we discuss the odd torque in the presence of shear strain. We choose the a- and b-axes as follows:

$$\begin{aligned}\mathbf{a} &= a \left( \cos \frac{\epsilon}{2}, \sin \frac{\epsilon}{2}, 0 \right)^T \\ \mathbf{b} &= a \left( \sin \frac{\epsilon}{2}, \cos \frac{\epsilon}{2}, 0 \right)^T,\end{aligned}\quad (24)$$

where we use  $\epsilon = 90^\circ - \gamma$  to quantify the shear strain, and  $\gamma$  is the angle between the a- and b-axes.

We present the axial tensors of rank 2 and rank 4 that are allowed by symmetry in shear-strained half-Heuslers in Table II. As indicated by arrows in the Table, tensors 6, 7, 15, 16, 17, and 18 do not need to be considered because both indices  $k$  and  $l$  of  $\chi_{ijkl}^{(a)}$  couple to magnetization in Eq. (3) and these tensors may therefore be replaced by others. Additionally, tensor 8 does not need to be considered, because it evaluates to zero when both indices  $k$  and  $l$  of  $\chi_{ijkl}^{(a)}$  are contracted with the magnetization. Tensor 1 describes the SOT effective field from Rashba SOI, tensors 2 describes the SOT effective field from Dresselhaus SOI [14], and the remaining tensors describe higher-order contributions that have not yet been discussed in the literature. Tensor 2 appears also in the case of tetragonal strain, see the first tensor in Table I. This is expected, because shear strain is automatically accompanied tetragonal strain.

The corresponding torkance may be written as

$$t_{ij}^{\text{odd}} = \sum_{\#}^2 \beta_{\#} \Xi_{im} \chi_{mj}^{(a\#)} + \sum_{\#}^{22} \beta_{\#} \Xi_{im} \chi_{mkl}^{(a\#)} \hat{M}_k \hat{M}_l, \quad (25)$$

where the matrix  $\Xi$  is defined in Eq. (10). As discussed above, one may set  $\beta_{\#} = 0$  for all tensors  $\#$  indicated by an arrow or by  $\emptyset$  in Table II, i.e.,  $\beta_6 = 0, \beta_7 = 0, \beta_8 = 0, \beta_{15} = 0, \dots$ . However, due to the relations

$$\begin{aligned}\Xi_{im} \chi_{mj}^{(a1)} &= \Xi_{im} \chi_{mkl}^{(a4)} \hat{M}_k \hat{M}_l - \Xi_{im} \chi_{mkl}^{(a12)} \hat{M}_k \hat{M}_l + \\ &+ \Xi_{im} \chi_{mkl}^{(a19)} \hat{M}_k \hat{M}_l + \Xi_{im} \chi_{mkl}^{(a21)} \hat{M}_k \hat{M}_l, \\ \Xi_{im} \chi_{mj}^{(a2)} &= \Xi_{im} \chi_{mkl}^{(a10)} \hat{M}_k \hat{M}_l + \Xi_{im} \chi_{mkl}^{(a20)} \hat{M}_k \hat{M}_l + \\ &+ \Xi_{im} \chi_{mkl}^{(a22)} \hat{M}_k \hat{M}_l, \\ \Xi_{im} \chi_{mj}^{(a3)} &= \Xi_{im} \chi_{mkl}^{(a10)} \hat{M}_k \hat{M}_l + \Xi_{im} \chi_{mkl}^{(a13)} \hat{M}_k \hat{M}_l, \\ \Xi_{im} \left[ \chi_{mkl}^{(a4)} - \Xi_{im} \chi_{mkl}^{(a9)} - \Xi_{im} \chi_{mkl}^{(a12)} \right] \hat{M}_k \hat{M}_l &= 0\end{aligned}\quad (26)$$

the remaining tensors in Eq. (25) are not linearly independent. Therefore, we may additionally choose  $\beta_{21} = 0, \beta_{22} = 0, \beta_{13} = 0$ , and  $\beta_{12} = 0$ . Thus, only 11 independent tensors need to be considered in Eq. (25) with 11 corresponding fitting parameters  $\beta_{\#}$ .

## B. Even torque

The effective field of the even torque can be expressed in terms of the electric field  $\mathbf{E}$  and the magnetization direction  $\hat{\mathbf{M}}$  as follows:

$$B_i^{\text{even}} = \chi_{ijk}^{(p)} E_j \hat{M}_k + \chi_{ijklm}^{(p)} E_j \hat{M}_k \hat{M}_l \hat{M}_m + \dots \quad (27)$$

Here,  $\chi_{ijk}^{(p)}$  is a polar tensor of third rank,  $\chi_{ijklm}^{(p)}$  is a polar tensor of fifth rank and summation over repeated indices is implied. Note that the effective field of the even torque is odd in the magnetization.

*Cubic PtMnSb*

In the absence of strain, i.e., when  $a = b = c$  and  $\alpha = \beta = \gamma = 90^\circ$ , symmetry allows 11 polar tensors of rank 3 and rank 5, which we list in Table III.

TABLE III. List of polar tensors of rank 3 and 5 allowed by symmetry in cubic half Heuslers. The notation introduced in Eq. (5) is used. Arrows indicate tensors that may be replaced by others.

#	$\chi^{(p\#)}$
1	$\langle 321 \rangle + \langle 231 \rangle + \langle 312 \rangle + \langle 132 \rangle + \langle 213 \rangle + \langle 123 \rangle$
2	$-\langle 13121 \rangle - \langle 12131 \rangle - \langle 23212 \rangle - \langle 21232 \rangle - \langle 32313 \rangle - \langle 31323 \rangle$
3	$\langle 32221 \rangle + \langle 23331 \rangle + \langle 31112 \rangle + \langle 13332 \rangle + \langle 21113 \rangle + \langle 12223 \rangle$
4	$\langle 31211 \rangle + \langle 21311 \rangle + \langle 32122 \rangle + \langle 12322 \rangle + \langle 23133 \rangle + \langle 13233 \rangle \rightarrow \chi^{(p3)}$
5	$\langle 32111 \rangle + \langle 23111 \rangle + \langle 31222 \rangle + \langle 13222 \rangle + \langle 21333 \rangle + \langle 12333 \rangle$
6	$\langle 13211 \rangle + \langle 12311 \rangle + \langle 23122 \rangle + \langle 21322 \rangle + \langle 32133 \rangle + \langle 31233 \rangle \rightarrow \chi^{(p2)}$
7	$\langle 23221 \rangle + \langle 32331 \rangle + \langle 31112 \rangle + \langle 31332 \rangle + \langle 12113 \rangle + \langle 21223 \rangle$
8	$\langle 11321 \rangle + \langle 11231 \rangle + \langle 22312 \rangle + \langle 22132 \rangle + \langle 33213 \rangle + \langle 33123 \rangle$
9	$-\langle 33321 \rangle - \langle 22231 \rangle - \langle 33312 \rangle - \langle 11132 \rangle - \langle 22213 \rangle - \langle 11123 \rangle \rightarrow \chi^{(p8)}$
10	$-\langle 31121 \rangle - \langle 21131 \rangle - \langle 32212 \rangle - \langle 12232 \rangle - \langle 23313 \rangle - \langle 13323 \rangle$
11	$-\langle 22321 \rangle - \langle 33231 \rangle - \langle 11312 \rangle - \langle 33132 \rangle - \langle 11213 \rangle - \langle 22123 \rangle$

In Eq. (27) the last three indices are contracted with the magnetization. Therefore, for the purpose of application in Eq. (27),  $\chi_{ijklm}^{(p6)}$  is equivalent with  $\chi_{ijklm}^{(p2)}$ ,  $\chi_{ijklm}^{(p4)}$  is equivalent with  $\chi_{ijklm}^{(p3)}$ , and  $\chi_{ijklm}^{(p9)}$  is equivalent with  $\chi_{ijklm}^{(p8)}$ , as indicated in the Table. Consequently, we do not need to consider  $\chi_{ijklm}^{(p6)}$ ,  $\chi_{ijklm}^{(p4)}$ , and  $\chi_{ijklm}^{(p9)}$ . Thus, the contribution to the effective field of the even SOT which is third order in  $\hat{\mathbf{M}}$  can be expressed in terms of the tensor

### Tetragonal strain

TABLE IV. List of polar tensors of rank 3 and 5 allowed by symmetry in tetragonally strained half Heuslers. The notation introduced in Eq. (5) is used. Arrows indicate tensors that may be replaced by others due to permutation of indices, while (29) denotes tensors that may be replaced by others due to Eq. (29).

#	$\chi^{(p\#)}$	#	$\chi^{(p\#)}$
1	$\langle 321 \rangle + \langle 312 \rangle$	18	$\langle 13121 \rangle + \langle 23212 \rangle \rightarrow 17$
2	$\langle 231 \rangle + \langle 132 \rangle$	19	$\langle 22321 \rangle + \langle 11312 \rangle \rightarrow 6$
3	$\langle 213 \rangle + \langle 123 \rangle$	20	$\langle 11321 \rangle + \langle 22312 \rangle \rightarrow 6$
4	$\langle 33231 \rangle + \langle 33132 \rangle$	21	$\langle 31211 \rangle + \langle 32122 \rangle \rightarrow 15$
5	$\langle 33321 \rangle + \langle 33312 \rangle \rightarrow 4$	22	$\langle 13211 \rangle + \langle 23122 \rangle \rightarrow 17$
6	$\langle 22231 \rangle + \langle 11132 \rangle$	23	$\langle 32111 \rangle + \langle 31222 \rangle \text{ (29)}$
7	$\langle 32331 \rangle + \langle 31332 \rangle$	24	$\langle 23111 \rangle + \langle 13222 \rangle \text{ (29)}$
8	$\langle 23331 \rangle + \langle 13332 \rangle$	25	$\langle 12311 \rangle + \langle 21322 \rangle \text{ (29)}$
9	$\langle 33213 \rangle + \langle 33123 \rangle \rightarrow 4$	26	$\langle 21311 \rangle + \langle 12322 \rangle \text{ (29)}$
10	$\langle 32313 \rangle + \langle 31323 \rangle \rightarrow 7$	27	$\langle 11231 \rangle + \langle 22132 \rangle \rightarrow 6$
11	$\langle 23313 \rangle + \langle 13323 \rangle \rightarrow 8$	28	$\langle 12131 \rangle + \langle 21232 \rangle \rightarrow 25$
12	$\langle 32133 \rangle + \langle 31233 \rangle \rightarrow 7$	29	$\langle 21131 \rangle + \langle 12232 \rangle \rightarrow 26$
13	$\langle 23133 \rangle + \langle 13233 \rangle \rightarrow 8$	30	$\langle 22213 \rangle + \langle 11123 \rangle \rightarrow 6$
14	$\langle 21333 \rangle + \langle 12333 \rangle$	31	$\langle 11213 \rangle + \langle 22123 \rangle \rightarrow 6$
15	$\langle 31121 \rangle + \langle 32212 \rangle$	32	$\langle 12113 \rangle + \langle 21223 \rangle \rightarrow 25$
16	$\langle 32221 \rangle + \langle 31112 \rangle \rightarrow 15$	33	$\langle 21113 \rangle + \langle 12223 \rangle \rightarrow 26$
17	$\langle 23221 \rangle + \langle 13112 \rangle \text{ (29)}$		

Next, we discuss the case of tetragonal strain. For  $a = b \neq c$  and  $\alpha = \beta = \gamma = 90^\circ$  we list the polar tensors that are allowed by symmetry in Table IV. In Eq. (27) the indices  $k, l$  and  $m$  of  $\chi_{ijklm}^{(p)}$  are contracted with the magnetization direction and are therefore interchangeable. Tensors that are related to other tensors by interchange of the indices  $k, l$  and  $m$  are specified in Table IV by arrows. These tensors do not need to be considered when we expand  $\chi_{ijklm}^{(p)}$ . When considering the permutations of the indices  $k, l$  and  $m$  the list of independent tensors that are needed in the expansion of  $\chi_{ijk}^{(p)}$  and  $\chi_{ijklm}^{(p)}$  is therefore reduced to the following ones: 1, 2, 3, 4, 6, 7, 8, 14, 15, 17, 23, 24, 25, 26.

Due to the relations

$$\begin{aligned} \Xi_{ni}[\chi_{ijklm}^{(p4)} + 2\chi_{ijklm}^{(p17)}]\hat{M}_k\hat{M}_l\hat{M}_m &= 0 \\ \Xi_{ni}[\chi_{ijklm}^{(p6)} + \chi_{ijklm}^{(p7)} + \chi_{ijklm}^{(p25)}]\hat{M}_k\hat{M}_l\hat{M}_m &= 0 \\ [\chi_{ijklm}^{(p7)} + \chi_{ijklm}^{(p15)} + \chi_{ijklm}^{(p23)}]\hat{M}_k\hat{M}_l\hat{M}_m &= \chi_{ijk}^{(p1)}\hat{M}_k \quad (29) \\ [\chi_{ijklm}^{(p8)} + \chi_{ijklm}^{(p17)} + \chi_{ijklm}^{(p24)}]\hat{M}_k\hat{M}_l\hat{M}_m &= \chi_{ijk}^{(p2)}\hat{M}_k \\ [\chi_{ijklm}^{(p14)} + \chi_{ijklm}^{(p25)} + \chi_{ijklm}^{(p26)}]\hat{M}_k\hat{M}_l\hat{M}_m &= \chi_{ijk}^{(p3)}\hat{M}_k \end{aligned}$$

we do not need to consider the tensors 17, 23, 24, 25, and 26. This leaves us with 3 polar tensors of rank 3 and 6 polar tensors of rank 5 to describe the SOT effective magnetic field in the tetragonal case, i.e., 9 tensors in total.

Using  $\mathbf{T}^{\text{even}} = \hat{\mathbf{M}} \times \mathbf{B}^{\text{even}}$ , and  $\mathbf{T}^{\text{even}} = \mathbf{t}^{\text{even}} \mathbf{E}$ , we

$$\begin{aligned} \chi_{ijklm}^{(p)} &= \alpha_2 \chi_{ijklm}^{(p2)} + \alpha_3 \chi_{ijklm}^{(p3)} + \alpha_5 \chi_{ijklm}^{(p5)} + \alpha_7 \chi_{ijklm}^{(p7)} \\ &+ \alpha_8 \chi_{ijklm}^{(p8)} + \alpha_{10} \chi_{ijklm}^{(p10)} + \alpha_{11} \chi_{ijklm}^{(p11)}. \end{aligned} \quad (28)$$

arrive at

$$t_{ij}^{\text{even}} = \mu \sum_{k=1}^9 \gamma_k \vartheta_{ij}^{(\text{even}k)} \quad (30)$$

with

$$\begin{aligned} \vartheta^{(\text{even}1)} &= \begin{pmatrix} \hat{M}_2^2 & \hat{M}_1 \hat{M}_2 & 0 \\ -\hat{M}_1 \hat{M}_2 & -\hat{M}_1^2 & 0 \\ 0 & 0 & 0 \end{pmatrix} \\ \vartheta^{(\text{even}2)} &= \begin{pmatrix} 0 & 0 & -\hat{M}_1 \hat{M}_3 \\ 0 & 0 & \hat{M}_2 \hat{M}_3 \\ 0 & 0 & -\hat{M}_2^2 + \hat{M}_1^2 \end{pmatrix} \\ \vartheta^{(\text{even}3)} &= \begin{pmatrix} -\hat{M}_3^2 & 0 & 0 \\ 0 & \hat{M}_3^2 & 0 \\ \hat{M}_1 \hat{M}_3 & -\hat{M}_2 \hat{M}_3 & 0 \end{pmatrix} \\ \vartheta^{(\text{even}4)} &= \begin{pmatrix} 0 & 0 & 2\hat{M}_1 \hat{M}_2^2 \hat{M}_3 \\ 0 & 0 & -2\hat{M}_1^2 \hat{M}_2 \hat{M}_3 \\ 0 & 0 & 0 \end{pmatrix} \\ \vartheta^{(\text{even}5)} &= \begin{pmatrix} 0 & -\hat{M}_1 \hat{M}_2 \hat{M}_3^2 & 0 \\ \hat{M}_1 \hat{M}_2 \hat{M}_3^2 & 0 & 0 \\ -\hat{M}_1 \hat{M}_2^2 \hat{M}_3 & \hat{M}_1^2 \hat{M}_2 \hat{M}_3 & 0 \end{pmatrix} \\ \vartheta^{(\text{even}6)} &= \begin{pmatrix} \hat{M}_2^2 \hat{M}_3^2 & \hat{M}_1 \hat{M}_2 \hat{M}_3^2 & 0 \\ -\hat{M}_1 \hat{M}_2 \hat{M}_3^2 & -\hat{M}_1^2 \hat{M}_3^2 & 0 \\ 0 & 0 & 0 \end{pmatrix} \\ \vartheta^{(\text{even}7)} &= \begin{pmatrix} 0 & 0 & -\hat{M}_3^3 \hat{M}_1 \\ 0 & 0 & \hat{M}_3^3 \hat{M}_2 \\ 0 & 0 & \hat{M}_1^2 \hat{M}_3^2 - \hat{M}_2^2 \hat{M}_3^2 \end{pmatrix} \\ \vartheta^{(\text{even}8)} &= \begin{pmatrix} -\hat{M}_3^4 & 0 & 0 \\ 0 & \hat{M}_3^4 & 0 \\ \hat{M}_3^3 \hat{M}_1 & -\hat{M}_3^3 \hat{M}_2 & 0 \end{pmatrix} \\ \vartheta^{(\text{even}9)} &= \begin{pmatrix} \hat{M}_1^2 \hat{M}_2^2 & \hat{M}_2^3 \hat{M}_1 & 0 \\ -\hat{M}_1^3 \hat{M}_2 & -\hat{M}_1^2 \hat{M}_2^2 & 0 \\ 0 & 0 & 0 \end{pmatrix}. \end{aligned} \quad (31)$$

### Shear strain

Finally, we consider the case of shear strain. In Table V we present the polar tensors of rank 3 and 5 allowed by symmetry in shear-strained half Heuslers. As indicated in the Table by arrows, several tensors may be replaced by others, because in Eq. (27) the indices  $k$ ,  $l$  and  $m$  of  $\chi_{ijklm}^{(\text{p})}$  are interchangeable.

TABLE V. List of polar tensors of rank 3 and 5 allowed by symmetry in shear-strained half Heuslers. The notation introduced in Eq. (5) is used. Arrows indicate tensors that may be replaced by others due to permutations of indices, while tensors indicated by (33) may be replaced by others due to Eq. (33).

#	$\chi^{(\text{p}\#)}$	#	$\chi^{(\text{p}\#)}$
1	$\langle 333 \rangle$	35	$\langle 12113 \rangle + \langle 21223 \rangle \rightarrow 21$
2	$\langle 231 \rangle + \langle 132 \rangle$	36	$\langle 11113 \rangle + \langle 22223 \rangle \rightarrow 22$
3	$\langle 321 \rangle + \langle 312 \rangle$	37	$\langle 13313 \rangle + \langle 23323 \rangle \rightarrow 27$
4	$\langle 311 \rangle + \langle 322 \rangle$	38	$\langle 23133 \rangle + \langle 13233 \rangle \rightarrow 14$
5	$\langle 131 \rangle + \langle 232 \rangle$	(33)	$\langle 13133 \rangle + \langle 23233 \rangle \rightarrow 27$
6	$\langle 213 \rangle + \langle 123 \rangle$	40	$\langle 21333 \rangle + \langle 12333 \rangle$ (33)
7	$\langle 113 \rangle + \langle 223 \rangle$	41	$\langle 11333 \rangle + \langle 22333 \rangle$ (33)
8	$\langle 21321 \rangle + \langle 12312 \rangle$	42	$\langle 32221 \rangle + \langle 31112 \rangle$
9	$\langle 22321 \rangle + \langle 11312 \rangle$	43	$\langle 31221 \rangle + \langle 32112 \rangle$
10	$\langle 21131 \rangle + \langle 12232 \rangle$	44	$\langle 32121 \rangle + \langle 31212 \rangle \rightarrow 43$
11	$\langle 22131 \rangle + \langle 11232 \rangle$	45	$\langle 31121 \rangle + \langle 32212 \rangle \rightarrow 42$
12	$\langle 21231 \rangle + \langle 12132 \rangle \rightarrow 8$	46	$\langle 33321 \rangle + \langle 33312 \rangle$ (33)
13	$\langle 22231 \rangle + \langle 11132 \rangle \rightarrow 9$	47	$\langle 32211 \rangle + \langle 31122 \rangle \rightarrow 43$
14	$\langle 23331 \rangle + \langle 13332 \rangle$	48	$\langle 31211 \rangle + \langle 32122 \rangle \rightarrow 42$
15	$\langle 13221 \rangle + \langle 23112 \rangle$	49	$\langle 32111 \rangle + \langle 31222 \rangle$ (33)
16	$\langle 13121 \rangle + \langle 23212 \rangle$	50	$\langle 31111 \rangle + \langle 32222 \rangle$ (33)
17	$\langle 12321 \rangle + \langle 21312 \rangle \rightarrow 8$	51	$\langle 33311 \rangle + \langle 33322 \rangle$ (33)
18	$\langle 11321 \rangle + \langle 22312 \rangle \rightarrow 9$	52	$\langle 33231 \rangle + \langle 33132 \rangle \rightarrow 46$
19	$\langle 13211 \rangle + \langle 23122 \rangle \rightarrow 16$	53	$\langle 33131 \rangle + \langle 33232 \rangle \rightarrow 51$
20	$\langle 13111 \rangle + \langle 23222 \rangle$	54	$\langle 32331 \rangle + \langle 31332 \rangle$ (33)
21	$\langle 12311 \rangle + \langle 21322 \rangle$	55	$\langle 31331 \rangle + \langle 32332 \rangle$ (33)
22	$\langle 11311 \rangle + \langle 22322 \rangle$	56	$\langle 33213 \rangle + \langle 33123 \rangle \rightarrow 46$
23	$\langle 12231 \rangle + \langle 21132 \rangle \rightarrow 8$	57	$\langle 33113 \rangle + \langle 33223 \rangle \rightarrow 51$
24	$\langle 11231 \rangle + \langle 22132 \rangle \rightarrow 9$	58	$\langle 32313 \rangle + \langle 31323 \rangle \rightarrow 54$
25	$\langle 12131 \rangle + \langle 21232 \rangle \rightarrow 21$	59	$\langle 31313 \rangle + \langle 32323 \rangle \rightarrow 55$
26	$\langle 11131 \rangle + \langle 22232 \rangle \rightarrow 22$	60	$\langle 32133 \rangle + \langle 31233 \rangle \rightarrow 54$
27	$\langle 13331 \rangle + \langle 23332 \rangle$ (33)	61	$\langle 31133 \rangle + \langle 32233 \rangle \rightarrow 55$
28	$\langle 21113 \rangle + \langle 12223 \rangle \rightarrow 10$	62	$\langle 33333 \rangle$ (33)
29	$\langle 22113 \rangle + \langle 11223 \rangle \rightarrow 11$	63	$\langle 23111 \rangle + \langle 13222 \rangle$ (33)
30	$\langle 21213 \rangle + \langle 12123 \rangle \rightarrow 8$	64	$\langle 23211 \rangle + \langle 13122 \rangle \rightarrow 15$
31	$\langle 22213 \rangle + \langle 11123 \rangle \rightarrow 9$	65	$\langle 21311 \rangle + \langle 12322 \rangle \rightarrow 10$
32	$\langle 23313 \rangle + \langle 13323 \rangle \rightarrow 14$	66	$\langle 22311 \rangle + \langle 11322 \rangle \rightarrow 11$
33	$\langle 12213 \rangle + \langle 21123 \rangle \rightarrow 8$	67	$\langle 23121 \rangle + \langle 13212 \rangle \rightarrow 15$
34	$\langle 11213 \rangle + \langle 22123 \rangle \rightarrow 9$	68	$\langle 23221 \rangle + \langle 13112 \rangle \rightarrow 16$

The corresponding torkance may be written as

$$t_{ij}^{\text{even}} = \Xi_{in} \left[ \sum_{\# = 1}^7 \beta_{\#} \chi_{njk}^{(\text{p}\#)} + \sum_{\# = 8}^{68} \beta_{\#} \chi_{njklm}^{(\text{p}\#)} \hat{M}_l \hat{M}_m \right] \hat{M}_k, \quad (32)$$

where the matrix  $\Xi$  is defined in Eq. (10). As discussed above, one may set  $\beta_{\#} = 0$  for all tensors  $\#$  indicated by an arrow in Table II, i.e.,  $\beta_{12} = 0$ ,  $\beta_{13} = 0$ ,  $\beta_{17} = 0$ ,  $\dots$ .

Due to the relations

$$\begin{aligned}
\Xi_{in} \chi_{njk}^{(p1)} \hat{M}_k &= \Xi_{in} [\chi_{njk\bar{l}m}^{(p51)} + \chi_{njk\bar{l}m}^{(p62)}] \hat{M}_k \hat{M}_l \hat{M}_m \\
\Xi_{in} \chi_{njk}^{(p1)} \hat{M}_k &= -\Xi_{in} \chi_{njk\bar{l}m}^{(p5)} \hat{M}_k \hat{M}_l \hat{M}_m \\
0 &= \Xi_{in} [\chi_{njk\bar{l}m}^{(p27)} + \chi_{njk\bar{l}m}^{(p62)}] \hat{M}_k \hat{M}_l \hat{M}_m \\
0 &= \Xi_{in} [\chi_{njk\bar{l}m}^{(p16)} + \frac{1}{2} \chi_{njk\bar{l}m}^{(p46)}] \hat{M}_k \hat{M}_l \hat{M}_m \\
0 &= \Xi_{in} \left[ \chi_{njk}^{(p1)} + [\chi_{njk\bar{l}m}^{(p15)} + \chi_{njk\bar{l}m}^{(p20)} + \chi_{njk\bar{l}m}^{(p27)}] \hat{M}_l \hat{M}_m \right] \hat{M}_k \\
0 &= \Xi_{in} \left[ \chi_{njk}^{(p2)} - [\chi_{njk\bar{l}m}^{(p14)} + \chi_{njk\bar{l}m}^{(p63)} - \frac{1}{2} \chi_{njk\bar{l}m}^{(p46)}] \hat{M}_l \hat{M}_m \right] \hat{M}_k \\
0 &= \Xi_{in} \left[ \chi_{njk}^{(p3)} - [\chi_{njk\bar{l}m}^{(p42)} + \chi_{njk\bar{l}m}^{(p49)} + \chi_{njk\bar{l}m}^{(p54)}] \hat{M}_l \hat{M}_m \right] \hat{M}_k \\
0 &= \Xi_{in} \left[ \chi_{njk}^{(p3)} + [\chi_{njk\bar{l}m}^{(p9)} + \chi_{njk\bar{l}m}^{(p21)} - \chi_{njk\bar{l}m}^{(p42)} \right. \\
&\quad \left. - \chi_{njk\bar{l}m}^{(p49)}] \hat{M}_l \hat{M}_m \right] \hat{M}_k \\
0 &= \Xi_{in} \left[ \chi_{njk}^{(p4)} - [\chi_{njk\bar{l}m}^{(p43)} + \chi_{njk\bar{l}m}^{(p50)} + \chi_{njk\bar{l}m}^{(p55)}] \hat{M}_l \hat{M}_m \right] \hat{M}_k \\
0 &= \Xi_{in} \left[ \chi_{njk}^{(p4)} + [\chi_{njk\bar{l}m}^{(p8)} + \chi_{njk\bar{l}m}^{(p22)} - \chi_{njk\bar{l}m}^{(p43)} \right. \\
&\quad \left. - \chi_{njk\bar{l}m}^{(p50)}] \hat{M}_l \hat{M}_m \right] \hat{M}_k \\
0 &= \Xi_{in} \left[ \chi_{njk}^{(p6)} - [\chi_{njk\bar{l}m}^{(p10)} + \chi_{njk\bar{l}m}^{(p21)} + \chi_{njk\bar{l}m}^{(p40)}] \hat{M}_l \hat{M}_m \right] \hat{M}_k \\
0 &= \Xi_{in} \left[ \chi_{njk}^{(p7)} - [\chi_{njk\bar{l}m}^{(p11)} + \chi_{njk\bar{l}m}^{(p22)} + \chi_{njk\bar{l}m}^{(p41)}] \hat{M}_l \hat{M}_m \right] \hat{M}_k
\end{aligned} \tag{33}$$

we may additionally set  $\beta_{\#} = 0$  in Eq. (32) for  $\# = 5, 27, 40, 41, 46, 49, 50, 51, 54, 55, 62, 63$ . Thus, there are only 6 linearly independent polar tensors of rank 3 and 12 linearly independent polar tensors of rank 5 that need to be considered in Eq. (32), i.e., 18 tensors in total and 18 corresponding fitting parameters  $\beta_{\#}$ .

### III. RESULTS

#### A. Computational details

We performed electronic structure calculations of PtMnSb based on the generalized gradient approximation (GGA) [25] as implemented in the FLEUR program [26]. In order to judge how sensitive the SOT is to the exchange correlation functional, we performed additional calculations within the local density approximation (LDA) [27]. The lattice constant of unstrained cubic PtMnSb is  $a_{\text{cub}} = c_{\text{cub}} = 11.72a_0$  in our calculations, where  $a_0$  is Bohr's radius. We considered 4 systems with different tetragonal strains  $\eta = (c - c_{\text{cub}})/c_{\text{cub}}$ :  $\eta = 1.45\%$  ( $a = 11.49a_0$  and  $c = 11.89a_0$ ),  $\eta = 0.723\%$  ( $a = 11.61a_0$  and  $c = 11.81a_0$ ),  $\eta = -0.723\%$  ( $a = 11.84a_0$  and  $c = 11.64a_0$ ), and  $\eta = -1.45\%$  ( $a = 11.95a_0$  and  $c = 11.55a_0$ ). Additionally, we considered 7 systems with different shear strains  $\epsilon = \gamma - 90^\circ$ , where  $\gamma$  is the angle between the  $a$  axis and the  $b$  axis:  $\epsilon = 2^\circ$ ,  $\epsilon = 1^\circ$ ,  $\epsilon = 0.5^\circ$ ,  $\epsilon = 0.2^\circ$ ,  $\epsilon = 0.1^\circ$ ,  $\epsilon = -0.1^\circ$ ,  $\epsilon = -0.2^\circ$

After obtaining the electronic structure self-consistently we generated maximally localized Wannier functions (MLWFs) using the Wannier90 code [28] in order to calculate the SOTs according to the method described in Ref. [29] with the help of Wannier interpolation for computational speed-up. We disentangled 44 MLWFs from 66 bands. For Mn and Pt we used  $sp^3d^2$ ,  $d_{xy}$ ,  $d_{yz}$  and  $d_{zx}$  trial orbitals. For Sb we employed  $s$  and  $p$  trial orbitals.

The even torkance is given by [29]

$$\begin{aligned}
t_{ij}^{\text{even}} &= \frac{e\hbar}{2\pi\mathcal{N}} \sum_{\mathbf{k}n \neq m} \text{Im} [\langle \psi_{\mathbf{k}n} | \mathcal{T}_i | \psi_{\mathbf{k}m} \rangle \langle \psi_{\mathbf{k}m} | v_j | \psi_{\mathbf{k}n} \rangle] \left\{ \right. \\
&\quad \frac{\Gamma(\mathcal{E}_{\mathbf{k}m} - \mathcal{E}_{\mathbf{k}n})}{[(\mathcal{E}_F - \mathcal{E}_{\mathbf{k}n})^2 + \Gamma^2] \left[ (\mathcal{E}_F - \mathcal{E}_{\mathbf{k}m})^2 + \Gamma^2 \right]} + \\
&\quad \left. + \frac{2\Gamma}{[\mathcal{E}_{\mathbf{k}n} - \mathcal{E}_{\mathbf{k}m}] \left[ (\mathcal{E}_F - \mathcal{E}_{\mathbf{k}m})^2 + \Gamma^2 \right]} + \right. \\
&\quad \left. + \frac{2}{[\mathcal{E}_{\mathbf{k}n} - \mathcal{E}_{\mathbf{k}m}]^2} \text{Im} \log \frac{\mathcal{E}_{\mathbf{k}m} - \mathcal{E}_F - i\Gamma}{\mathcal{E}_{\mathbf{k}n} - \mathcal{E}_F - i\Gamma} \right\}
\end{aligned} \tag{34}$$

and the odd torkance is given by

$$t_{ij}^{\text{odd}} = \frac{e\hbar}{\pi\mathcal{N}} \sum_{\mathbf{k}nm} \frac{\Gamma^2 \text{Re} [\langle \psi_{\mathbf{k}n} | \mathcal{T}_i | \psi_{\mathbf{k}m} \rangle \langle \psi_{\mathbf{k}m} | v_j | \psi_{\mathbf{k}n} \rangle]}{[(\mathcal{E}_F - \mathcal{E}_{\mathbf{k}n})^2 + \Gamma^2] \left[ (\mathcal{E}_F - \mathcal{E}_{\mathbf{k}m})^2 + \Gamma^2 \right]}, \tag{35}$$

where  $\mathcal{N}$  is the number of  $\mathbf{k}$ -points used to sample the Brillouin zone,  $e$  is the elementary positive charge,  $\mathcal{T}_i$  is the  $i$ -th Cartesian component of the torque operator,  $v_j$  is the  $j$ -th Cartesian component of the velocity operator,  $\Gamma$  is the quasiparticle broadening, and  $\psi_{\mathbf{k}n}$  and  $\mathcal{E}_{\mathbf{k}n}$  denote the Bloch function for band  $n$  at  $k$ -point  $\mathbf{k}$  and the corresponding band energy, respectively. A constant broadening of  $\Gamma = 25$  meV was used in the calculations unless noted otherwise.

Due to the half-metallicity the spin magnetic moment per unit cell takes the integer value  $\mu = 4\mu_B$  when SOI is not included in the calculations, where  $\mu_B$  is Bohr's magneton. In our calculations of SOT we include SOI and therefore the magnetic moment slightly deviates from the integer value  $\mu = 4\mu_B$ . This deviation depends on the strain, but it is at most 1% for the strains that we consider. Therefore,  $\mu \approx 4\mu_B$  is very well satisfied in all our calculations. When we present our *ab-initio* results we use  $ea_0 \approx 8.478 \times 10^{-30}$  Cm as the unit of torkance. A torkance of one  $ea_0$  corresponds therefore to an effective magnetic field of  $B = ea_0 E / \mu \approx 0.229$   $\mu$ T when the applied electric field is  $E = 1$  V/m.

In Ref. [29] we have shown that the odd SOT is proportional to  $1/\Gamma$  in the limit  $\Gamma \rightarrow 0$ , while the even SOT is independent of  $\Gamma$  in this limit. Therefore, it may be convenient to discuss the odd SOT per applied electric current, because this ratio is independent of  $\Gamma$  in the limit of  $\Gamma \rightarrow 0$ . The resistivity of unstrained cubic PtMnSb at  $\Gamma = 25$  meV is given by  $\rho_{xx} = 17\mu\Omega\text{cm}$ . Consequently, an odd torkance of one  $ea_0$  at  $\Gamma = 25$  meV corresponds to an

effective magnetic field per electric current-density ratio of  $B/j = ea_0 E/(\mu j) = ea_0 \rho_{xx}/\mu \approx 3.89 \times 10^{-14} \text{ Tm}^2/\text{A}$ .

## B. Odd torque

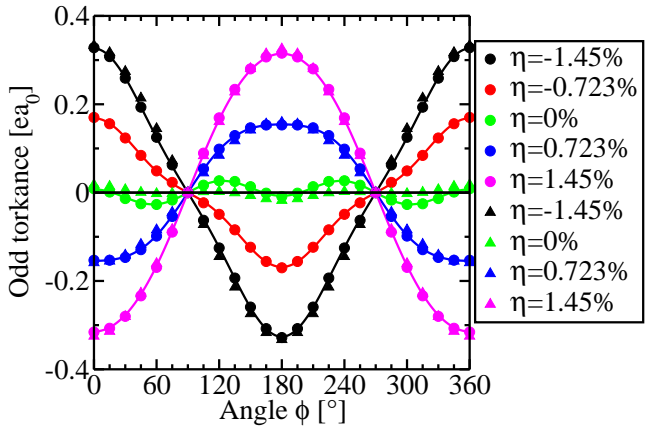


FIG. 1. Angular dependence of the odd torkance in PtMnSb for several strains  $\eta = (c - c_{\text{cub}})/c_{\text{cub}}$  obtained in GGA (filled circles) and LDA (filled triangles) when the electric current is applied along [110] direction and when the magnetization is in-plane.  $\phi$  is the angle between the magnetization and the [110] direction. The component of the odd torque pointing in [001] direction is shown. Solid lines are fits to the GGA results according to Eq. (15).

In Fig. 1 we show the odd torkance as a function of the azimuthal angle of the magnetization for different tetragonal strains. Strain increases the odd torkance significantly. In the strained systems the differences between the torkances computed with GGA (filled circles) and LDA (filled triangles) are very small. However, in the unstrained system GGA and LDA differ even qualitatively: Here, the torkance has maxima close to 120° and close to 240° when GGA is used. However, when LDA is used it has a maximum at 0° instead. When we use Eq. (15) to fit the *ab-initio* results we obtain very good agreement between the fit and the data, as shown in the figure.

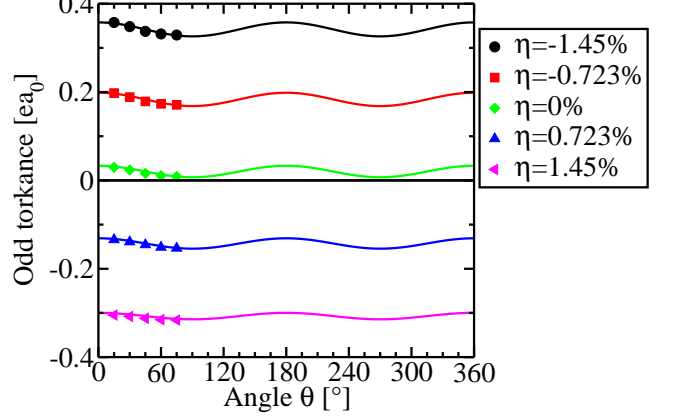


FIG. 2. Angular dependence of the odd torkance in PtMnSb for several strains  $\eta = (c - c_{\text{cub}})/c_{\text{cub}}$  obtained in GGA when the electric current is applied in [110] direction. The magnetization is rotated from [001] direction ( $\theta=0$ ) to [110] direction ( $\theta = 90^\circ$ ). We show only the component of the torque that is parallel to the unit vector  $e_\theta$  of the spherical coordinate system. *Ab-initio* data are shown by symbols, while solid lines are fits according to Eq. (15).

In Fig. 2 we show the odd torkance as a function of the polar angle  $\theta$ . It varies only moderately with the angle  $\theta$ , in contrast to the strong variation with the angle  $\phi$  shown in Fig. 1. When the tetragonal strain is  $\eta = 1.45\%$  the odd torkance is of the same order of magnitude as the even and odd torkances in magnetic bilayers such as Co/Pt and Mn/W [29].

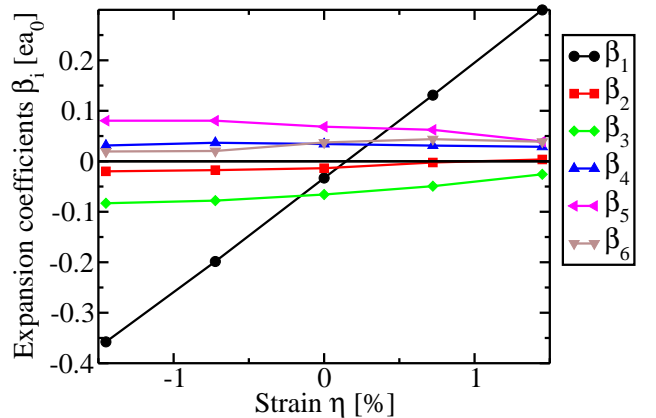


FIG. 3. PtMnSb: Expansion coefficients  $\beta_i$  in Eq. (15) for several strains  $\eta = (c - c_{\text{cub}})/c_{\text{cub}}$  when the odd torkance is obtained from GGA.

In Fig. 3 we show the strain-dependence of the parameters  $\beta_k$  in Eq. (15), which we use to fit the *ab-initio* results. In cubic PtMnSb we find that the relations Eq. (23)

are satisfied well. The coefficient  $\beta_1$  varies linearly with strain and depends strongly on it, while the coefficients  $\beta_2$  through  $\beta_6$  are less sensitive to strain than  $\beta_1$ . In Eq. (15)  $\beta_1$  is the coefficient of  $\vartheta_{ij}^{(\text{odd}1)}$ , which describes the SOT from Dresselhaus-type SOI. However,  $\beta_1$  does not vanish for zero strain. Of course, this does not imply that there is a Dresselhaus field at  $\eta = 0$ . Instead, it is simply a manifestation of Eq. (14), which shows that  $\vartheta_{ij}^{(\text{odd}1)}$  is not linearly independent from the higher order contributions described by the tensors 2, 3, 5, and 7.

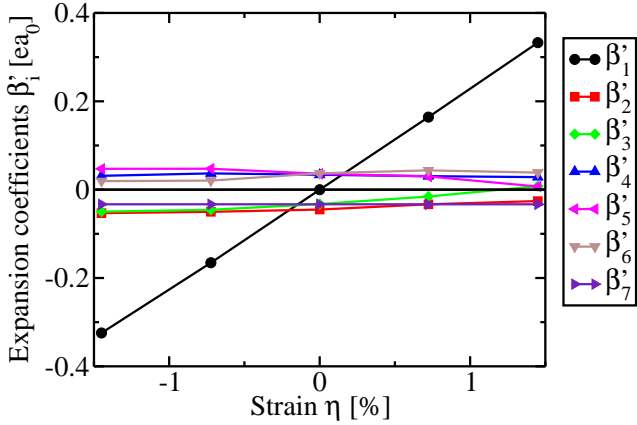


FIG. 4. PtMnSb: Expansion coefficients  $\beta'_i$  in Eq. (36) for several strains  $\eta = (c - c_{\text{cub}})/c_{\text{cub}}$  when the odd torkance is obtained from GGA.

In Eq. (15) we made the choice  $\alpha_7=0$  in order to get an unambiguous representation of the torque in terms of a set of fitting parameters, which is only possible when we expand the torkance in terms of linearly independent tensors. However, it is possible to choose a different combination of tensors such that the coefficient of  $\vartheta_{ij}^{(\text{odd}1)}$  is zero at  $\eta = 0$ . Such a combination has the advantage that one may claim that the coefficient of  $\vartheta_{ij}^{(\text{odd}1)}$  corresponds to the Dresselhaus SOI. For this purpose we perform a second fitting run after determining the parameters  $\beta_1, \dots, \beta_6$  in Eq. (15) in the first fitting run. The second fitting run is based on

$$t_{ij}^{\text{odd}} = \sum_{k=1}^7 \beta'_k \vartheta_{ij}^{(\text{odd}k)}, \quad (36)$$

where we fix  $\beta'_7 = \beta_1(\eta = 0)$ , while  $\beta'_1, \dots, \beta'_6$  are free fitting parameters. As shown in Fig. 4 this two-step fitting procedure leads to  $\beta'_1(\eta = 0) = 0$ , which can be understood easily from Eq. (14). We can thus claim that  $\beta'_1$  describes the SOT from the Dresselhaus field.

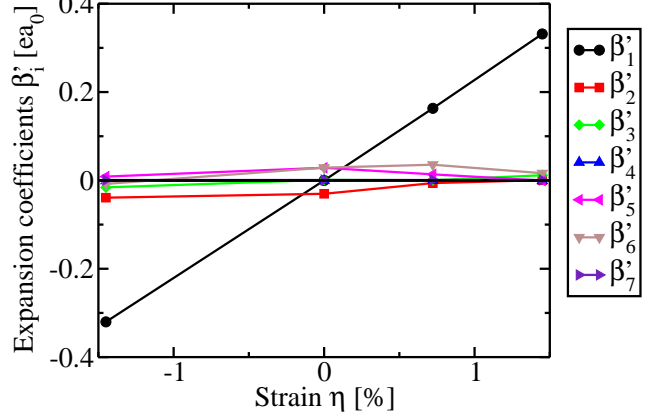


FIG. 5. PtMnSb: Expansion coefficients  $\beta'_i$  in Eq. (36) for several strains  $\eta = (c - c_{\text{cub}})/c_{\text{cub}}$  when the odd torkance is obtained from LDA.

In Fig. 5 we show the expansion coefficients for the SOT obtained from LDA. Interestingly, the  $\beta'_1$  in Fig. 4 and Fig. 5 differ by less than 1%. Thus, the differences between LDA and GGA, which are illustrated in Fig. 1, are reflected mostly by the differences in the higher-order coefficients  $\beta'_2, \dots, \beta'_7$ . These higher-order coefficients differ significantly between GGA and LDA. However, for sufficiently large strain the contribution of the higher-order terms is relatively small compared with the Dresselhaus SOT described by  $\beta'_1$ . Therefore, the odd SOT is insensitive to the choice of the exchange correlation potential in strained PtMnSb, as discussed already in Fig. 1.

Next, we discuss the effect of shear strain  $\epsilon$  on the odd torque. In Fig. 6 we show the odd torkance as a function of the azimuthal angle  $\phi$  in the shear strained crystal. The enhancement of the odd SOT with shear strain is similarly strong as the enhancement with tetragonal strain. When the shear strain is  $\epsilon = 2^\circ$  the odd torkance is of the same order of magnitude as the even and odd torkances in magnetic bilayers such as Co/Pt and Mn/W [29]. The variation of the odd torkance with azimuthal angle  $\phi$  is similar to the angular dependence in tetragonally strained PtMnSb shown in Fig. 1.

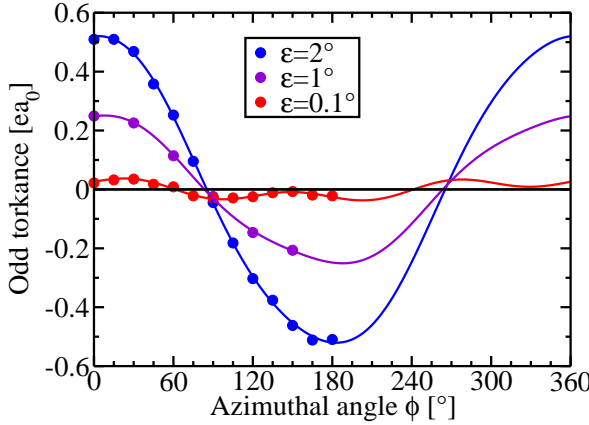


FIG. 6. Odd torkance in shear-strained PtMnSb obtained in GGA. The current direction is along [100]. The magnetization is in-plane.  $\phi$  is the angle between the magnetization and the [100] direction. *Ab-initio* data are shown by filled circles, while solid lines are fits according to Eq. (25).

At  $\epsilon = 2^\circ$  the odd torkance exhibits a maximum at  $\phi = 0^\circ$ . In order to investigate the dependence of this maximum on  $\epsilon$  we show in Fig. 7 the odd torkance at  $\phi = 0^\circ$  as a function of  $\epsilon$ . In the considered range the dependence on  $\epsilon$  is approximately linear.

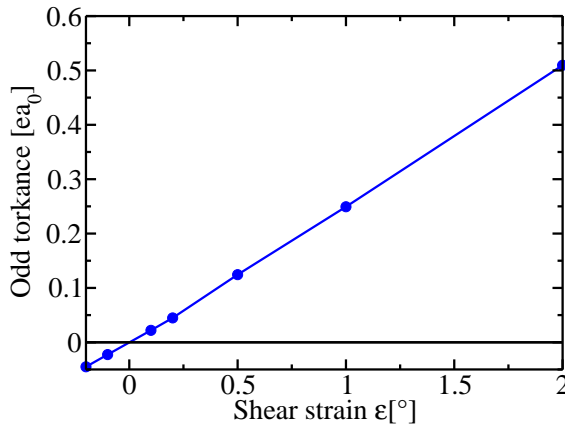


FIG. 7. Dependence of the odd torkance on shear-strain in PtMnSb when the polar and azimuthal angles of magnetization are  $\theta = 90^\circ$  and  $\phi = 0^\circ$ , respectively.

In Fig. 8 we show the expansion coefficients  $\beta_i$  in Eq. (25) of the odd torkance. At large shear strain  $\beta_1$  dominates clearly over the other contributions, i.e., the SOT from Rashba SOI is dominant. Since shear strain automatically implies tetragonal strain, a SOT from Dresselhaus SOI – described by  $\beta_2$  – is present as well, but it is small compared to the SOT from Rashba

SOI.

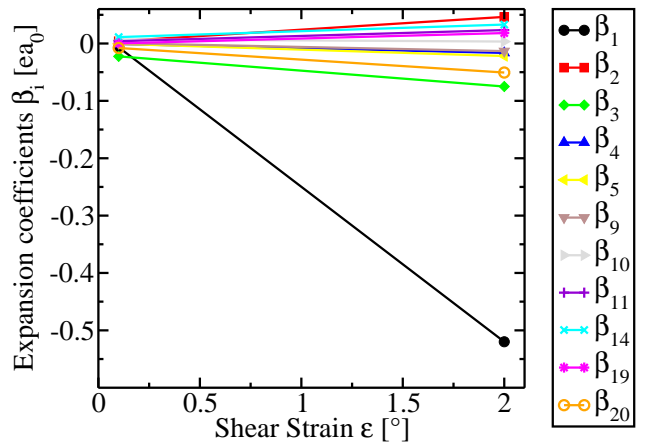


FIG. 8. Expansion coefficients  $\beta_i$  in Eq. (25) of the odd torkance in shear-strained PtMnSb obtained in GGA.

### C. Even Torque

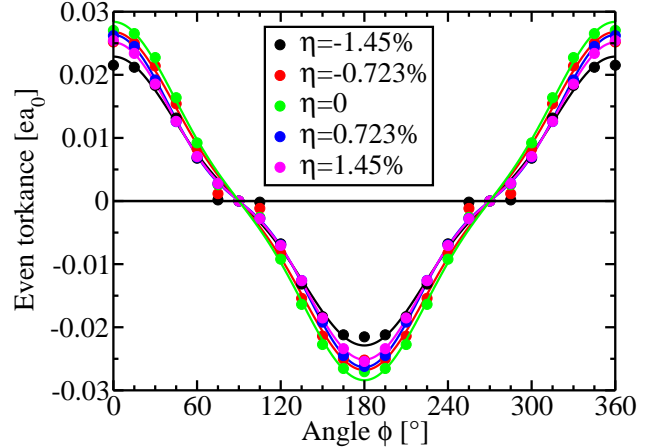


FIG. 9. Angular dependence of the even torkance obtained within GGA in PtMnSb for several tetragonal strains  $\eta = (c - c_{\text{cub}})/c_{\text{cub}}$  when the electric current is applied along [110] direction and when the magnetization is in-plane.  $\phi$  is the angle between magnetization and the [110] direction. We show the component of the even torque that is parallel to the unit vector  $e_\phi$  of the spherical coordinate system. *Ab-initio* data are shown by filled circles, while solid lines are fits according to Eq. (30).

In Fig. 9 we show the even torkance as a function of the azimuthal angle  $\phi$  for several tetragonal strains  $\eta$ . The even torque is considerably less sensitive to strain than the odd torque. Additionally, at  $\eta = 1.45\%$  the maximum even torkance is smaller than the maximum odd

torkance by a factor of 12.5. In contrast to magnetic bilayer systems such as Co/Pt [15], where the even SOT is typically more important than the odd SOT, in PtMnSb the odd SOT dominates.

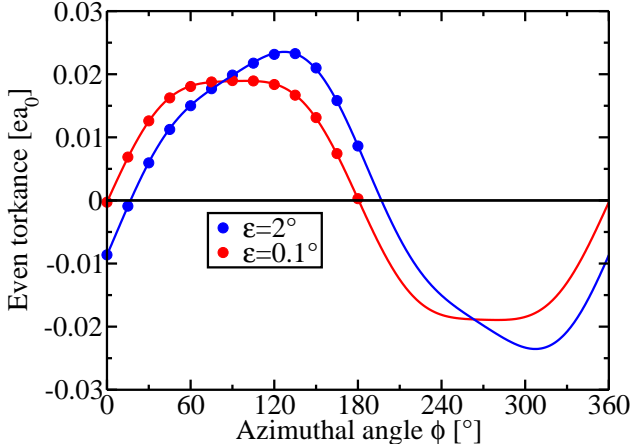


FIG. 10. Angular dependence of the even torkance obtained within GGA in PtMnSb for several shear strains  $\epsilon$  when the electric current is applied along [100] direction and when the magnetization is in-plane.  $\phi$  is the angle between magnetization and the [100] direction. We show the component of the even torque that is parallel to the unit vector  $e_\phi$  of the spherical coordinate system. *Ab-initio* data are shown by filled circles, while solid lines are fits according to Eq. (32).

In Fig. 10 we show the even torkance in shear-strained PtMnSb at  $\Gamma = 100$  meV. While the even torkance is more sensitive to shear strain than to tetragonal strain, it is less sensitive to shear strain than the odd torkance.

#### IV. SUMMARY

We discuss the constraints that crystal symmetry imposes on the form of the SOT torkance tensor in half

Heuslers with tetragonal or shear strain. We discuss the lowest order tensors, which correspond to Rashba and Dresselhaus SOI, but also higher order tensors. We perform first principles DFT calculations of the SOT in half-Heusler PtMnSb as a function of tetragonal and shear strain. The odd torkance in PtMnSb depends strongly on tetragonal strain, which we attribute to the Dresselhaus SOI. We find the SOT from Dresselhaus SOI to be insensitive to the exchange-correlation functional, i.e., the differences between GGA and LDA are negligible. In contrast, the higher-order tensors differ substantially between GGA and LDA. However, these higher-order contributions are small in PtMnSb with tetragonal strain, such that the total odd torque in PtMnSb is insensitive to the exchange-correlation functional. The even torkance depends only weakly on tetragonal strain, but it depends moderately strong on shear strain. The dependence of the odd SOT on shear strain is similarly strong as its dependence on tetragonal strain and it arises mostly from Rashba SOI.

#### ACKNOWLEDGMENTS

We acknowledge financial support from Leibniz Collaborative Excellence project OptiSPIN – Optical Control of Nanoscale Spin Textures, and funding under SPP 2137 “Skyrmionics” of the DFG. We gratefully acknowledge financial support from the European Research Council (ERC) under the European Union’s Horizon 2020 research and innovation program (Grant No. 856538, project “3D MAGiC”). The work was also supported by the Deutsche Forschungsgemeinschaft (DFG, German Research Foundation) – TRR 173 – 268565370 (project A11), TRR 288 – 422213477 (project B06). We also gratefully acknowledge the Jülich Supercomputing Centre and RWTH Aachen University for providing computational resources under project No. jiff40.

---

[1] A. Manchon, J. Železný, I. M. Miron, T. Jungwirth, J. Sinova, A. Thiaville, K. Garello, and P. Gambardella, Current-induced spin-orbit torques in ferromagnetic and antiferromagnetic systems, *Rev. Mod. Phys.* **91**, 035004 (2019).

[2] I. Galanakis, P. Mavropoulos, and P. H. Dederichs, Electronic structure and slater-pauling behaviour in half-metallic heusler alloys calculated from first principles, *Journal of Physics D: Applied Physics* **39**, 765 (2006).

[3] K. Elphick, W. Frost, M. Samiepour, T. Kubota, K. Takanashi, S. Hiroaki, S. Mitani, and A. Hirohata, Heusler alloys for spintronic devices: review on recent development and future perspectives, *Science and Technology of Advanced Materials* 10.1080/14686996.2020.1812364 (2020).

[4] J. Ma, V. I. Hegde, K. Munira, Y. Xie, S. Keshavarz, D. T. Mildebrath, C. Wolverton, A. W. Ghosh, and W. H. Butler, Computational investigation of half-Heusler compounds for spintronics applications, *Phys. Rev. B* **95**, 024411 (2017).

[5] F. Casper, T. Graf, S. Chadov, B. Balke, and C. Felser, Half – Heusler compounds: novel materials for energy and spintronic applications, *Semiconductor Science and Technology* **27**, 063001 (2012).

[6] B. Kwon, Y. Sakuraba, H. Sukegawa, S. Li, G. Qu, T. Furubayashi, and K. Hono, Anisotropic magnetoresistance and current-perpendicular-to-plane giant magnetoresistance in epitaxial NiMnSb-based multilayers,

Journal of Applied Physics **119**, 023902 (2016).

[7] Z. Wen, T. Kubota, T. Yamamoto, and K. Takanashi, Enhanced current-perpendicular-to-plane giant magnetoresistance effect in half-metallic NiMnSb based nanojunctions with multiple Ag spacers, *Applied Physics Letters* **108**, 232406 (2016).

[8] G. Qu, P.-H. Cheng, Y. Du, Y. Sakuraba, S. Kasai, and K. Hono, Investigation of spin-dependent transports and microstructure in NiMnSb-based magnetoresistive devices, *Applied Physics Letters* **111**, 222402 (2017).

[9] Z. Wen, T. Kubota, T. Yamamoto, and K. Takanashi, Fully epitaxial c1b-type NiMnSb half-Heusler alloy films for current-perpendicular-to-plane giant magnetoresistance devices with a Ag spacer, *Scientific Reports* **5**, 18387 (2015).

[10] C. Liu, C. K. A. Mewes, M. Chshiev, T. Mewes, and W. H. Butler, Origin of low gilbert damping in half metals, *Applied Physics Letters* **95**, 022509 (2009).

[11] C. Ciccarelli, L. Anderson, V. Tshitoyan, A. J. Ferguson, F. Gerhard, C. Gould, L. W. Molenkamp, J. Gayles, J. Zelezny, L. Smejkal, Z. Yuan, J. Sinova, F. Freimuth, and T. Jungwirth, Room-temperature spin-orbit torque in NiMnSb, *Nature physics* **12**, 855 (2016).

[12] J. Železný, Z. Fang, K. Olejník, J. Patchett, F. Gerhard, C. Gould, L. W. Molenkamp, C. Gomez-Olivella, J. Zemen, T. Tichý, T. Jungwirth, and C. Ciccarelli, Unidirectional magnetoresistance and spin-orbit torque in NiMnSb (2021), arXiv:2102.12838 [cond-mat.mes-hall].

[13] N. Zhao, A. Sud, H. Sukegawa, S. Komori, K. Rogdakis, K. Yamanoi, J. Patchett, J. W. A. Robinson, C. Ciccarelli, and H. Kurebayashi, Growth, strain, and spin-orbit torques in epitaxial Ni – Mn – Sb films sputtered on GaAs, *Phys. Rev. Materials* **5**, 014413 (2021).

[14] J. Železný, H. Gao, A. Manchon, F. Freimuth, Y. Mokrousov, J. Zemen, J. Mašek, J. Sinova, and T. Jungwirth, Spin-orbit torques in locally and globally noncentrosymmetric crystals: Antiferromagnets and ferromagnets, *Phys. Rev. B* **95**, 014403 (2017).

[15] K. Garello, I. M. Miron, C. O. Avci, F. Freimuth, Y. Mokrousov, S. Blügel, S. Auffret, O. Boulle, G. Gaudin, and P. Gambardella, Symmetry and magnitude of spin-orbit torques in ferromagnetic heterostructures, *Nature Nanotech.* **8**, 587 (2013).

[16] F. Mahfouzi and N. Kioussis, First-principles study of the angular dependence of the spin-orbit torque in Pt/Co and Pd/Co bilayers, *Phys. Rev. B* **97**, 224426 (2018).

[17] J.-P. Hanke, F. Freimuth, B. Dupé, J. Sinova, M. Kläui, and Y. Mokrousov, Engineering the dynamics of topological spin textures by anisotropic spin-orbit torques, *Phys. Rev. B* **101**, 014428 (2020).

[18] K. D. Belashchenko, A. A. Kovalev, and M. van Schilfgaarde, First-principles calculation of spin-orbit torque in a Co/Pt bilayer, *Phys. Rev. Materials* **3**, 011401 (2019).

[19] J. Krieft, J. Mendil, M. H. Aguirre, C. O. Avci, C. Klewe, K. Rott, J.-M. Schmalhorst, G. Reiss, P. Gambardella, and T. Kuschel, Co-sputtered PtMnSb thin films and PtMnSb/Pt bilayers for spin-orbit torque investigations, *physica status solidi (RRL) - Rapid Research Letters* **11**, 1600439 (2018).

[20] M. C. Kautzky and B. M. Clemens, Structure and magneto-optical properties of epitaxial PtMnSb(001) on W(001)/MgO(001), *Applied Physics Letters* **66**, 1279 (1995).

[21] P. G. van Engen, K. H. J. Buschow, R. Jongebreur, and M. Erman, PtMnSb, a material with very high magneto-optical kerr effect, *Applied Physics Letters* **42**, 202 (1983).

[22] V. N. Antonov, P. M. Oppeneer, A. N. Yaresko, A. Y. Perlov, and T. Kraft, Computationally based explanation of the peculiar magneto-optical properties of PtMnSb and related ternary compounds, *Phys. Rev. B* **56**, 13012 (1997).

[23] M. C. Kautzky, F. B. Mancoff, J.-F. Bobo, P. R. Johnson, R. L. White, and B. M. Clemens, Investigation of possible giant magnetoresistance limiting mechanisms in epitaxial PtMnSb thin films, *Journal of Applied Physics* **81**, 4026 (1997).

[24] Z. Wen, T. Kubota, and K. Takanashi, Optimization of half-Heusler PtMnSb alloy films for spintronic device applications, *Journal of Physics D: Applied Physics* **51**, 435002 (2018).

[25] J. P. Perdew, K. Burke, and M. Ernzerhof, Generalized gradient approximation made simple, *Phys. Rev. Lett.* **77**, 3865 (1996).

[26] See <http://www.flapw.de>.

[27] U. von Barth and L. Hedin, A local exchange-correlation potential for the spin polarized case. i, *Journal of Physics C: Solid State Physics* **5**, 1629 (1972).

[28] G. Pizzi, V. Vitale, R. Arita, S. Blügel, F. Freimuth, G. Géranton, M. Gibertini, D. Gresch, C. Johnson, T. Koretsune, and et al., Wannier90 as a community code: new features and applications, *J. Phys.: Condens. Matter* **32**, 165902 (2020).

[29] F. Freimuth, S. Blügel, and Y. Mokrousov, Spin-orbit torques in Co/Pt(111) and Mn/W(001) magnetic bilayers from first principles, *Phys. Rev. B* **90**, 174423 (2014).